Accurate Determination of Optimal Amount of Charger Capacitors for PHEVs

R. Eslami*

Asistant Professor, Faculty of Electrical Engineering, Sahand University of Technology, Tabriz, Iran

ABSTRACT: Nowadays, because of the need to decrease fuel consumption and greenhouse gas emissions and also their capability of exchanging power with the grid and regulating the frequency and voltage of the grid at different times of the day, electric vehicles are used more than before all across the world. It is highly important to pay attention to the efficiency, and decrease in the weight and volume of these vehicles. The chargers of these vehicles can form a huge portion of the volume and weight of these vehicles. DC link capacitors are the large parts of these chargers. Based on the mathematical modeling and relationships of the system, this study focuses on the optimal capacitor value based on the required specifications. In the model presented in this article, the optimal value of DC link capacitor is estimated by taking into account instantaneous input power of the charger, the relationship of the energy balance between the grid and the DC link capacitor, and application of Taylor series to the output of the relationship. The optimal DC link capacitor value is estimated through calculating the DC link voltage, and measuring the exchanged energy and changes of DC Link Voltage during charging. The most considerable advantages of the proposed model are the simplicity of its design together with the minimum weight and volume of the charger due to its low capacitor value. SIMULINK environment of MATLAB software was used to evaluate the proposed model. The simulation results show that the model was successful.

1. Introduction

Nowadays, due to the urgent need to decrease fuel consumption and greenhouse gases emission, a lot of attention is paid to technologies of Electric Vehicles (EV) and Plug-in Hybrid Electric Vehicles (PHEV) [1-3]. Because the gasoline of PHEVs can be used as a secondary source of energy, these vehicles are used for long distances. Furthermore, their connectivity to power grid provides opportunities such as ancillary services, support and reactive power compensation, connectivity to renewable energy sources, and load balancing. The increased use of PHEVs allows these vehicles to be used as controllable loads to improve grid parameters [4]. Since the use of electric vehicles is very important in improving the power quality and reliability of the network, the operational standards of these vehicles have been prepared [5, 6]. However, different factors may impinge on the faster and more expansion of these vehicles; the high cost and life cycle of the batteries, charging operation complexities, the lack of charger infrastructure, and the harmful harmonic effects the battery chargers may have on power distribution systems [7, 8]. On the other hand, chargers with the capability of active control can decrease these damaging effects.

There are two groups of battery chargers for electric vehicles: on-Board and off-Board chargers with unidirectional

*Corresponding author's email: eslami@sut.ac.ir

and bidirectional power flows. The unidirectional charging systems constrain hardware requirements and simplify the issue of internal connectivity. They decrease battery erosion as well [8, 9]. On the other hand, bidirectional charging systems support grid charging, inject battery energy into the grid and stabilize the power by changing the power flow direction [10, 11]. Built-in chargers usually do not support high power because of the increase in weight, volume and cost [12]. These systems are either inductive or conductive. Conductive charging systems employ direct contact between the interface and the charger input, while inductive chargers transmit power magnetically.

The need to design protective circuits with the goal of preventing overcurrent and voltage surges is a major challenge in designing the chargers of electric vehicles [13]. For this purpose, the mechanism of most chargers is in accordance with Fig. 1. As shown in Fig. 1, constant current charging is used for low charge levels, and after the voltage reaches the maximum nominal of it, it is charged in constant voltage until the battery is fully charged.

High volume, high weight, low power, long charging time and harmonic output are the major challenges of the battery chargers for Plug-in Hybrid Electric Vehicles (PHEV) [14]. In a PHEV battery charger, the major part of the volume is the DC link capacitor [15]. Therefore, specifying the minimum
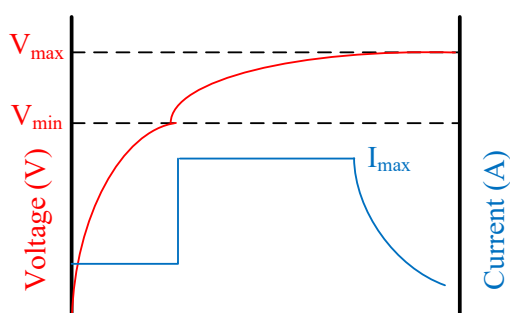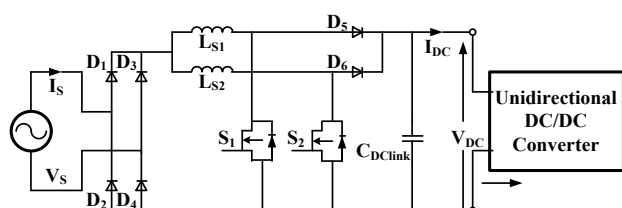
Fig. 1. Battery charging process for PHEVs

Fig. 2. Unidirectional charger topology with interleaved control method

capacitance that will decrease the charger volume will be very important in decreasing the volume and weight of these vehicles. Recently, bidirectional chargers have been used to employ PHEVs as distributed generations [14]. There is also a second frequency oscillation in the DC link voltage, which is caused by the second frequency oscillation in single-phase AC systems. This oscillation is very detrimental to batteries and should be removed by a filter in order to have a proper stability control system [15].

In this way, [16] presents a new method to reduce DC-link capacitor current ripple by decreasing the harmonics of the current waveform. Therefore the delivered useful power to the grid is increased within a low harmonic content. Since the DC-Link current ripple causes heat losses and the life of the capacitor and the system reliability is reduced, [17] presents a method to optimize DC-Link ripple in three level inverters for photovoltaic systems. None of the above studies had worked on reducing the volume of the DC-Link capacitor.

A single-phase, full-bridge built-in charger is used in this study to charge the electric vehicles. Due to their simplicity and effective performance, they are of great interest to manufacturers. As discussed earlier, size and weight are two of the major challenges in making electric vehicle chargers. Since DC link capacitors are the heaviest and the largest elements of single-phase chargers, this research uses precise mathematical equations to calculate the optimal DC link capacitors. Using these equations, the capacitor with the smallest value will be found. It will naturally have the least weight and volume. In addition, by optimally selecting the capacitor value, the harmonics of the charger input current and DC link voltage decrease to an acceptable level. As a result, the total harmonic distortions (THD) of these two waveforms are much lower than their standard values. It is necessary to

mention that the method suggested for estimating the value of DC link capacitors has a very simple process and design, which is another advantage of the model. Furthermore, the high precision of the proposed model and design is another advantage of the proposed model due to its reliance on precise mathematical relationships (not optimization algorithms). The simulation results also confirm the optimization of the proposed model in determining the capacitor. In addition, the designed control system enjoys appropriate dynamics that closely follows the DC link voltage changes.

The contents of the paper are as follow: In the second part, electric vehicles chargers are discussed and the topologies of unidirectional and bidirectional chargers are illustrated. In the third part, the proposed method of this paper for the charger design is presented and the optimal magnitude of the DC link capacitor of the charger is obtained. In the fourth part, the simulation results are given and are analyzed and finally in the last part of this paper a brief conclusion about the proposed method and its results are presented.

2. Hybrid Vehicles Chargers

Battery chargers have a vital role in the expansion of electric vehicles. Charging time and battery life are closely tied to the battery charger features. The battery charger must be efficient and reliable with high power capacity. They should also have low cost, volume and weight. Charger performance also relies on components, control system and switching strategies.

Electric vehicle chargers have a boost convertor to modify the power factor [18]. This design uses a diode bridge to rectify the input voltage, which is completed by the boost section. Based on boost converter and without bridge, the power factor correction (PFC) topology decreases the need for a rectifier input bridge, but still maintains the converter performance [19]. This converter overcomes the heat management issue in the rectifier diode input bridge, which is inherently involved in the conventional amplification of PFC. However, it raises electromagnetic interference (EMI). Previous studies also show that the interleaving control method decreases the battery ripple current and the inductor size [20, 21]. The unidirectional conFiguration shown in Fig. 2 consists of two parallel boost converters that have 180 degrees of phase difference [22]. An interlayer boost converter has the advantages of paralleled semiconductors. In this structure, in addition to removing the output ripple, the output capacitors stress will also be eliminated. Similar to boost converters, this topology should provide heat management for the input bridge rectifier, thus it is limited to a maximum power level of 3.5 kW [23]. Therefore, the bridgeless interleaved topology for power levels above 3.5 kW has been proposed in [24].

Currently, the majority of PHEVs use internal single-phase chargers for recharging their batteries.

2-1- Unidirectional chargers

Fig. 3 shows the unidirectional power flow between electric vehicles and the power grid. As shown in the charging arrows in Fig. 3, electric vehicles with unidirectional chargers
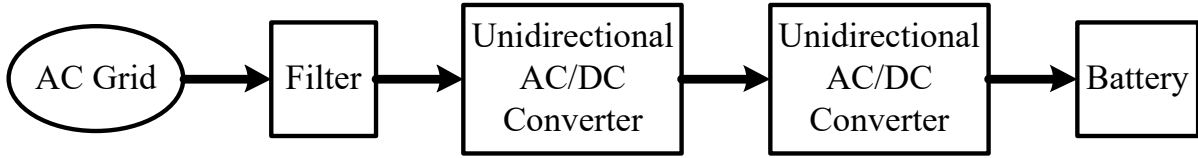
Fig. 3. The process of transferring electrical power in unidirectional chargers from the grid to the electric vehicle
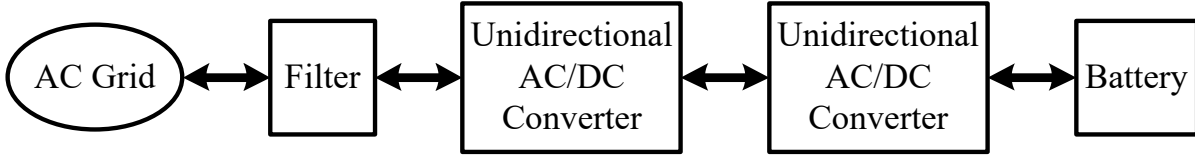

Fig. 4. The process of transferring electrical power in bidirectional chargers between the grid and the electric vehicle
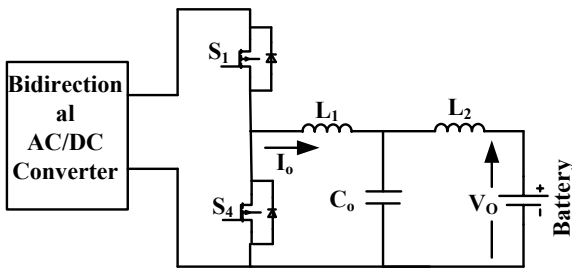

Fig. 5. Bidirectional non-isolated two-quarter chargers

can only charge their batteries through the grid, but they can never place their energy into the grid. These chargers usually use a diode bridge with a filter and DC-DC converter. Today, these converters are used in a single floor to reduce cost, weight, volume and waste.

2-2- Bidirectional chargers

In the bidirectional charger, as shown in Fig. 4, and contrary to the unidirectional charger, it is possible to discharge the vehicle's battery power over the power grid.

Conventional bidirectional chargers have two phases. One phase is an AC-DC converter connected to the bidirectional power grid, which compensates for power factor. The other phase is a bidirectional DC-DC converter current controller that regulates the battery current. These chargers may also employ isolated or non-isolated circuits.

When chargers are operating in charging mode, they must absorb the sinusoidal current at a defined phase angle to control the active and reactive power. In discharge mode, the charger must return the current in the same sinusoidal form. The bidirectional charger can support network charging, vehicle-to-grid power injection (V2G) and power stabilization. The topology shown in Fig. 5 is the bidirectional two-quadrant non-insulated charger. This circuit includes two switches that simplify circuit control. But there are two high-current inductors in the structure that are large and expensive, which can reduce in one direction and boosting role in the other direction.

The topology of Fig. 6 is the dual active bidirectional isolated charger. Although this structure provides high power capacity and fast control, its large number of elements results in a great increase in cost.

3. Suggested Model for Charger Design

A single-phase charger model consisting of a two-leg full-bridge converter is used in this study to design the charger. As shown in the charger circuit model illustrated in Fig. 7, a resistor paralleled with key is provided for the launch moment to prevent the flow of instantaneous current values. Using a parallel-reverse diode, in this charger at the moment of initial launch, the converter acts as a diode bridge, charging the DC link capacitor. There is also a series inductor with converter which is used to remove the switching harmonics caused by the converter and to prevent these harmonics from entering the grid. There is also a DC capacitor at the output of the charger that is responsible for saving energy and preventing instantaneous voltage changes. The load is parallel to these capacitors, which can also play the role of a convertor.

3-1- Determining optimum capacitor for DC Link of Charger (C_{dc})

In single-phase systems, particularly in single-phase chargers, the input instantaneous power can be estimated through Eq. (1).

$$\begin{aligned} P_{in} &= V_s * I_s = V_m \sin(\omega t) * I_m \sin(\omega t) \\ &= \frac{V_m I_m}{2} + \frac{V_m I_m}{2}\cos(2\omega t) = \bar{P}_{in} + \tilde{P}_{in} \end{aligned} \tag{1}$$

According to Eq. (1), the first part ($\bar{P}_{in}$) is constant power and the second part ($\tilde{P}_{in}$) is an oscillating component with a frequency twice higher than the network. In order to achieve a low DC voltage pulse, which is very important for batteries, the voltage pulse must be compensated with a capacitor in the DC link. Many studies have attempted to make this capacitor smaller to include less volume and weight in the electric
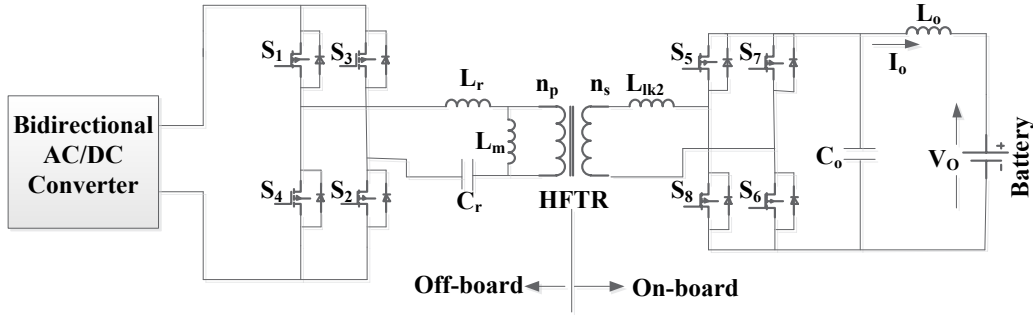
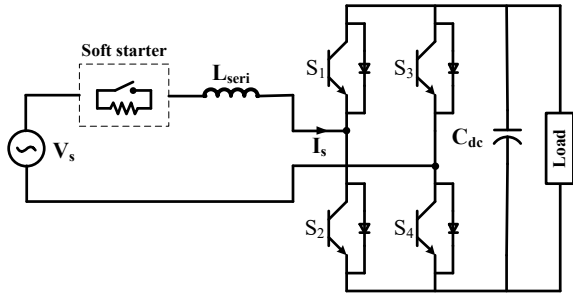**Fig. 6. Isolated bidirectional Dual charger**

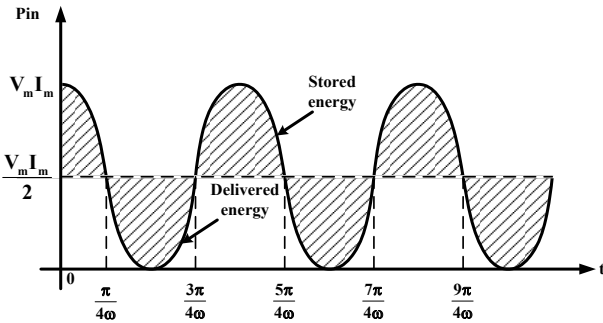**Fig. 7. The structure of the IGBT-based single phase charger**

Fig. 8. Power flow in DC link capacitor

vehicle. In this single-phase system, the energy balance between the grid and the capacitor can be written as Eq. (2).

$$\frac{1}{2}C_{dc}(V_{dc}^2(t)-V_o^2)=\int_o^t \frac{V_m I_m}{2}\cos(2\omega\tau)d\tau \tag{2}$$

By solving Eq. (2), applying Taylor series and neglecting the high frequency components, the DC link voltage will be estimated in terms of time and in the form of Eq. (3).

$$V_{dc}(t)=V_o+\frac{V_m I_m \sin(2\omega t)}{4\omega C_{dc} V_o}=V_o+\frac{\overline{P}_{in}\sin(2\omega t)}{2\omega C_{dc} V_o} \tag{3}$$

In this equation, V_0 is the mean DC link voltage.

Based on the maximum and minimum DC link voltage ($V_{dc,\max}$ and $V_{dc,\max}$) and as shown in Fig. 8, the energy

exchanged during the charging will be calculated according to Eq. (4).

$$\Delta E=\frac{1}{2}C_{dc}(V_{dc,\max}^2-V_{dc,\min}^2) \tag{4}$$

The mean value of DC link voltage is estimated through Eq. (5).

$$V_o=\frac{V_{dc,\max}+V_{dc,\min}}{2} \tag{5}$$

Furthermore, Eq. (6) also shows the DC link voltage ripple value.

$$\Delta V_{dc}=V_{dc,\max}-V_{dc,\min} \tag{6}$$

Based on Eqs. (3-6), the ripple amplitude of the DC link voltage will be obtained according to Eq. (7).

$$\Delta V_{dc}=V_{dc,\max}-V_{dc,\min}=\frac{\overline{P}_{in}}{\omega C_{dc} V_o} \tag{7}$$

Given that $\Delta V_{dc}<(\beta\%)\times V_o$, the value of the DC link capacitor could be estimated based on Eq. (8), where â is determined based on the pulse value tolerated by the DC-DC converter. Given this value and considering the power required to charge the batteries of hybrid electric vehicles, it is possible to calculate the optimum capacitor values. It should be noted that this value is minimal, which decreases the charger weight and size relatively well. On the other hand, it is also worth noting that for a built-in charger, magnetic and storage elements are the heaviest and most bulky parts, so the most valuable advantage of the proposed method in this paper is the definite answer to the problem and not using an optimal answer obtained from optimization methods.

$$C_{dc} \geq \frac{100\times\overline{P}_{in}}{\beta\omega V_o^2} \tag{8}$$

226

3-2- Control algorithm

In steady state of a three-phase system, the reference current in the synchronous reference device is DC value, yet in a single-phase system, the reference current is an AC current (with frequency of 50 Hz or 60 Hz). Therefore, one can assume that a current controller bandwidth in single-phase systems should be large enough to cover 50 Hz frequency. Due to limitations such as sampling effect, discretization, etc., too much gain can lead to instability, and furthermore the controller bandwidth cannot be easily expanded. This study used resonance controllers to control the reference current with high precision without the need to increase the bandwidth or the gain. As shown in Fig.9 , the structure of the proposed method uses a DC link voltage controller as the outer control loop and a current controller as the inner loop. The DC link voltage controller is an ordinary PI controller that is the reference current range (I_a^*). As shown in Eq. (9), the general reference current is obtained by multiplying reference current range (I_a^*) by the signal with the same phase of the grid voltage $\cos(\theta)$.

$$I_s^* = \cos(\hat{\theta}) \times (PI)\left(V_{dc}^* - V_{dc}\right) = I_a^* \cos(\hat{\theta}) \qquad (9)$$

The current controller is implemented based on a proportional-resonant controller whose conversion function is given in Eq. (10), in which K_r and K_p are respectively the gains of proportional and resonant controllers, and ω is the basic angular frequency of the source current.

$$G_r(s) = K_p + \frac{K_r 2_s}{s^2 + \omega^2} \qquad (10)$$

4. Simulation Results

In order to validate the proposed control system, simulations are applied to the structure presented in Fig. 9 in MATLAB / SIMULINK software. Table 1 shows the details of the simulated system. It is important to state that the different parameters pertinent to the charger, including voltages and currents, were investigated in the transient and steady state, and the results are presented in the section below.

4-1- The steady state of related voltages and currents of the charger

The results of the steady-state charger simulation are shown in Figures 10, 11 and 12. In this case, the charger has passed its transient state and all values have become steady. As discussed earlier, there is a second-frequency oscillation in the DC link voltage that is a result of the second-frequency oscillation in single-phase AC systems. This oscillation is very harmful to the batteries, thus a filter should be used to remove it.

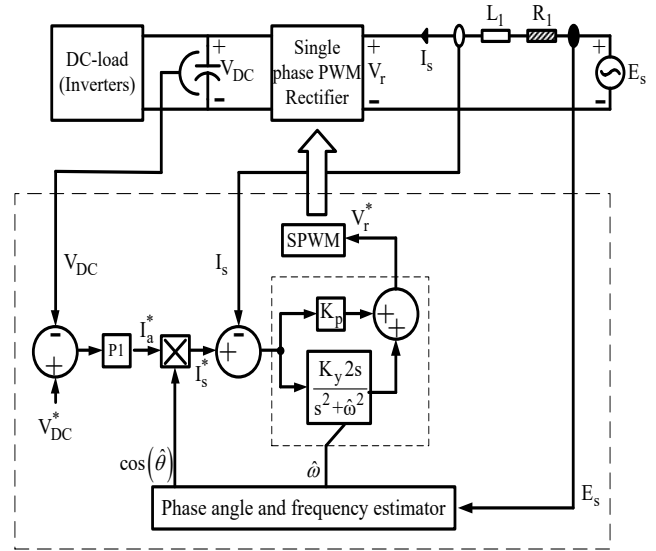As Fig. 10 shows, the maximum voltage waveform in the

Fig. 9. Control structure of the IGBT-based single-phase charger

Table 1. Simulated system specifications

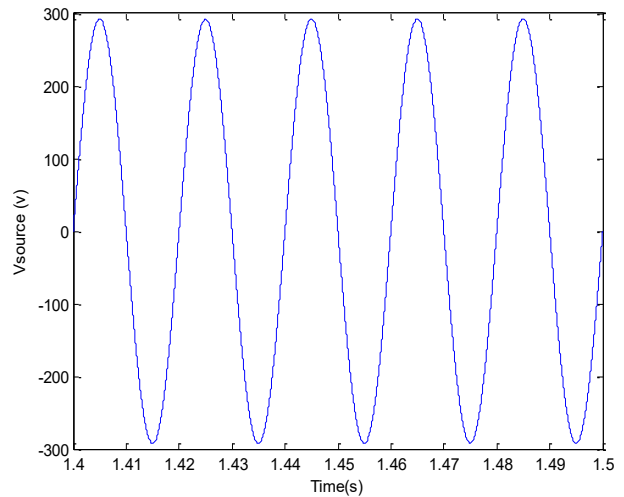| Parameter	Value
P_{in}	4kW
V_{in}	220V
V_{DC}	480V
L_{Seri}	7mH
C_{DC}	3300μF
$F_{Switching}$	3KHz
$F_{sampling}$	12KHz

Fig. 10. The voltage steady state waveform of the AC network side of the charger

steady state was about *290V*. Furthermore, according to the results of the calculations for harmonics, the voltage waveform of the AC grid side was acceptable and the produced THD voltage is less than *1%*.

In the case of the charger input waveforms, as shown in Fig. 11, the steady-state waveform amplitude is about *26A* and THD is about *4.37%*, which is acceptable.

According to Fig. 12, the DC link voltage is about *482V* with a ripple range of less than *10V* which is less than *3%* , therefore these results from the simulation of the proposed method are quite acceptable.

As discussed earlier, a very simple and straightforward equation was used to estimate the optimal value of charger capacitor in Eqs. (1) and (8). According to the estimated values given in Table 1 and the value of $\hat{a}=2$, the optimal value for the charger input capacitor will be obtained as Eq. (11).

$$C_{dc} \geq 2800\,\mu F \tag{11}$$

The optimum capacitor value is selected according to the standard values available in the market. Fig. 13 shows the value of the ripple voltage which confirms the achieved equation for the capacitor value.

As Fig. 13 shows, with the capacitor selected in Eq. (11), the DC link voltage ripple has decreased substantially within the acceptable range.

4-2- The transient state of related voltages and currents of the charger

This section presents the simulation results of the transient state of the DC link voltage parameters and the input current from the grid to the charger (Figures 14 and 15), which was a result of a change in DC load.

As Fig. 14 shows, the changes in the transient mode of the input current has increased from *20A* to about *35A* in *0.1s*, and after *0.1s*, the stability of the current waveform is completely maintained.

Although the ripple voltage increased, as shown in Fig. 15 and regarding the transient waveforms of DC link, yet it reached stability with *475V* and with a ripple value of less than *3%* over a short time (*0.3s*). Thus, according to the simulation results presented here, it can be stated that the control system follows the reference values of the voltage properly given step changes in the load or load voltage, and it is also safe to say that the system enjoys good dynamics.

5. Conclusion

This study is focused on different types of chargers used for rechargeable electric vehicles. As pointed out earlier, the chargers are divided into two types of built-in and external ones with unidirectional and bidirectional power charging flow. Built-in chargers, as a major component of electric vehicles, must have a very low size and weight in order to improve the general performance of the vehicles. This research presents a simple equation for estimating optimum value of DC link capacitors in these chargers, based on the modeling of a full bridge single-phase charger. Not only does this equation simplify the design, but it also gives the designer an optimum value for the weight and the volume, which decreases harmful effects in the waveform of the voltage and charger currents.
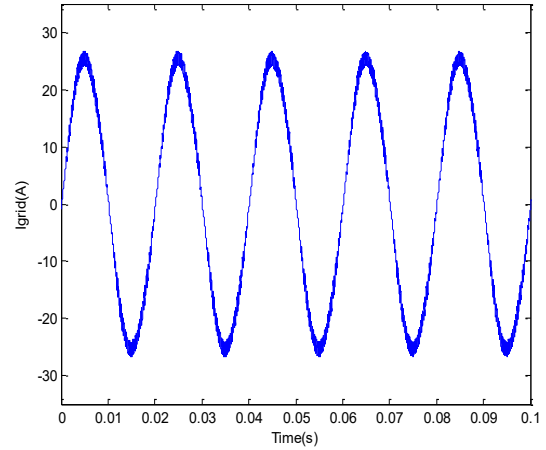

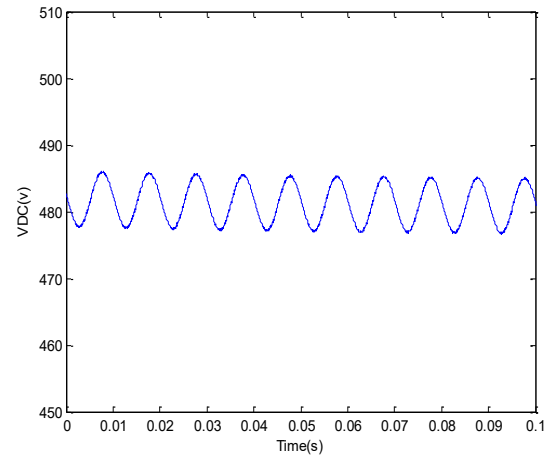**Fig. 11. The steady state waveform of the input current of the charger**

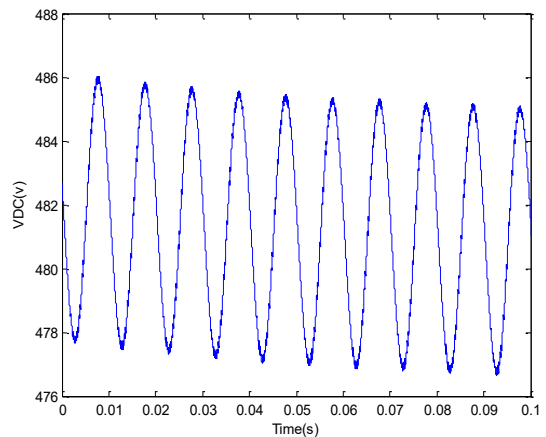**Fig. 12. The Voltage Waveform of the charger DC Link**

Fig. 13. The Voltage ripple of the charger DC Link

Simulations in MATLAB confirmed the proposed method for designing DC charger link capacitors. In addition to the steady state response, the control system presented in this paper also follows the transient states created with proper dynamics and maintains system stability.
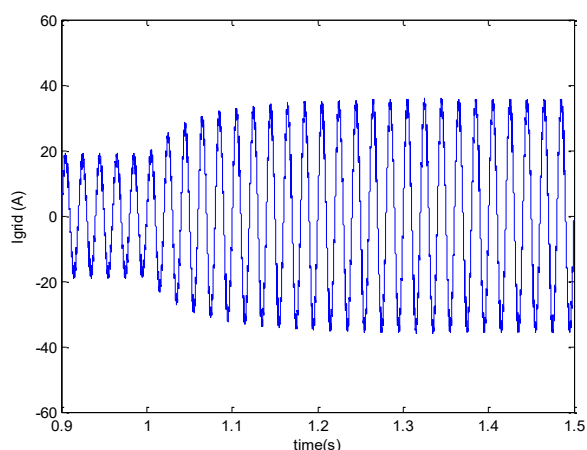
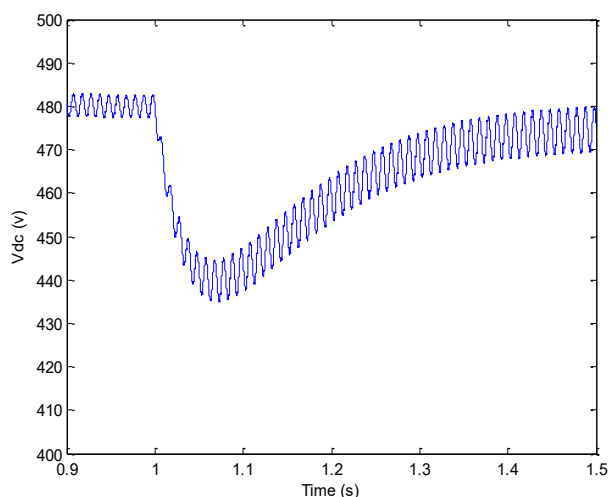**Fig. 14. The network current waveform due to the sudden shift in the load at 1s**

Fig. 15. The DC link voltage waveform due to the sudden shift in the load at 1s

6. References

[1] z. b, z. c, c. g, and z. b, "Electrical Vehicle Path Tracking Based Model Predictive Control with a Laguerre Function and Exponential Weight," *IEEE Access,* pp. 1-1, 2019.

[2] M. Ye, X. Song, R. Xiong, and F. Sun, "A Novel Dynamic Performance Analysis and Evaluation Model of Series-parallel Connected Battery Pack for Electric Vehicles," *IEEE Access,* pp. 1-1, 2019.

[3] J. Larminie, *Electric Vehicle Technology Explained*: Wiley, 2003.

[4] S. Han, S. Han, and K. Sezaki, "Development of an Optimal Vehicle-to-Grid Aggregator for Frequency Regulation," *IEEE Transactions on Smart Grid,* vol. 1, pp. 65-72, 2010.

[5] M. R. Khalid, M. S. Alam, A. Sarwar, and M. S. Jamil Asghar, "A Comprehensive review on electric vehicles charging infrastructures and their impacts on power-quality of the utility grid," *eTransportation,* vol. 1, p. 100006, 2019/08/01/ 2019.

[6] H. S. Das, M. M. Rahman, S. Li, and C. W. Tan, "Electric vehicles standards, charging infrastructure, and impact on grid integration: A technological review," *Renewable and Sustainable Energy Reviews,* vol. 120, p. 109618, 2020/03/01/ 2020.

[7] C. C. Chan and K. T. Chau, "An overview of power electronics in electric vehicles," *IEEE Transactions on Industrial Electronics,* vol. 44, pp. 3-13, 1997.

[8] B. Singh, B. N. Singh, A. Chandra, K. Al-Haddad, A. Pandey, and D. P. Kothari, "A review of three-phase improved power quality AC-DC converters," *IEEE Transactions on Industrial Electronics,* vol. 51, pp. 641-660, 2004.

[9] M. A. Fasugba and P. T. Krein, "Gaining vehicle-to-grid benefits with unidirectional electric and plug-in hybrid vehicle chargers," in *2011 IEEE Vehicle Power and Propulsion Conference*, 2011, pp. 1-6.

[10] X. Zhou, S. M. Lukic, S. Bhattacharya, and A. Huang, *Design and control of grid-connected converter in bi-directional battery charger for Plug-in hybrid electric vehicle application*, 2009.

[11] Z. Xiaohu, W. Gangyao, S. Lukic, S. Bhattacharya, and A. Huang, "Multi-function bi-directional battery charger for plug-in hybrid electric vehicle application," in *2009 IEEE Energy Conversion Congress and Exposition*, 2009, pp. 3930-3936.

[12] M. Grenier, M. G. H. Aghdam, and T. Thiringer, "Design of on-board charger for plug-in hybrid electric vehicle," in *5th IET International Conference on Power Electronics, Machines and Drives (PEMD 2010)*, 2010, pp. 1-6.

[13] V. Chitransh, A. Singh, and R. K. Singh, "A clamped feedback based digital versatile optimal bidirectional battery charger for HEV/PHEV," in *2015 IEEE 11th International Conference on Power Electronics and Drive Systems*, 2015, pp. 1138-1143.

[14] R. Razi, B. Asaei, and M. R. Nikzad, "A new battery charger for plug-in hybrid electric vehicle application using back to back converter in a utility connected micro-grid," in *2017 8th Power Electronics, Drive Systems & Technologies Conference (PEDSTC)*, 2017, pp. 13-18.

[15] L. Xue, D. Boroyevich, and P. Mattavelli, "Switching condition and loss modeling of GaN-based dual active bridge converter for PHEV charger," in *2016 IEEE Applied Power Electronics Conference and Exposition (APEC)*, 2016, pp. 1315-1322.

[16] A. Turksoy, Y. Hames, A. Teke, and M. B. Latran, "A novel adaptive switching method to reduce DC-Link capacitor ripple in PV based grid-connected inverter," *Solar Energy,* vol. 173, pp. 702-714, 2018.

[17] S. Kim, I. J. Won, J. Kim, and K. Lee, "DC-Link Ripple Current Reduction Method for Three-Level Inverters With Optimal Switching Pattern," *IEEE Transactions on Industrial Electronics,* vol. 65, pp. 9204-9214, 2018.

[18] H. Chang and C. Liaw, "Development of a Compact Switched-Reluctance Motor Drive for EV Propulsion With Voltage-Boosting and PFC Charging Capabilities," *IEEE Transactions on Vehicular Technology,* vol. 58, pp. 3198-3215, 2009.

[19] M. Budhia, G. A. Covic, J. T. Boys, and C. Huang, "Development and evaluation of single sided flux couplers for contactless electric vehicle charging," in *2011 IEEE Energy Conversion Congress and Exposition*, 2011, pp. 614-621.

[20] K. W. Klontz, A. Esser, P. J. Wolfs, and D. M. Divan, "Converter selection for electric vehicle charger systems with a high-frequency high-power link," in *Proceedings of IEEE Power Electronics Specialist Conference - PESC '93*, 1993, pp. 855-861.

[21] K. Throngnumchai, T. Kai, and Y. Minagawa, "A study on receiver circuit topology of a cordless battery charger for electric vehicles," in *2011 IEEE Energy Conversion Congress and Exposition*, 2011, pp. 843-850.

[22] A. W. Green and J. T. Boys, "10 kHz inductively coupled power transfer-concept and control," in *1994 Fifth International Conference on Power Electronics and Variable-Speed Drives*, 1994, pp. 694-699.

[23] J. T. Boys, G. A. Covic, and A. W. Green, "Stability and control of inductively coupled power transfer systems," *IEE Proceedings - Electric Power Applications,* vol. 147, pp. 37-43, 2000.

[24] P. Sergeant and A. V. D. Bossche, "Inductive coupler for contactless power transmission," *IET Electric Power Applications,* vol. 2, pp. 1-7, 2008.